Strain Rate-dependent Deformation and Failure Process of Adhesive Joints

M. Johar, S.F.M. Asasaari and *M.N. Tamin
Faculty of Mechanical Engineering
Universiti Teknologi Malaysia
81310 UTM Skudai, Johor, Malaysia
*e-mail: taminmn@fkm.utm.my, ph. +6012 7781 410

Abstract

Rate-dependent deformation and failure process of adhesive joints are investigated in this study. For this purpose, acrylic foam pressure sensitive adhesive (PSA) was employed with aluminum adherents. Tensile and shear loading of the adhesive joint was applied at displacement rates ranging from 5 to 500 mm/min. Results show that the failure process under tensile loadings start with initiation of cavities, hardening through fibrillation process and final fracture of the fibrils. For shear loading the failure process is a combination of fibrillation processes, shear flow, and by interfacial sliding. Both modulus and strain energy density at fracture reach maximum value at a displacement rate of 100 mm/min under tension, while continuously increase with displacement rate under shear loading. Adhesive failure dominates at low loading rate (below 10 mm/min.), while mixed-mode and cohesive failure are common at faster loading rates above 250 mm/min. Finite element employing Yeoh constitutive model adequately predicts viscous shear deformation of the PSA joints.

Keywords: Pressure-sensitive adhesive, adhesive joint, interface strength, strain-rate dependent, finite element simulation

1. Introduction

Pressure-sensitive adhesive (PSA) forms the desired bond or joint between the adherents when relatively light pressure is applied. Initial contact between the adhesive and adherents is accomplished by elastic and possibly viscous deformation of the material under low external stresses [1]. While wetting establishes the adhesion, van der Waals's forces give rise to the strength of the joint. PSA was found in numerous applications in electronic and packaging industry including Electromagnetic Interference (EMI) shielding and grounding of electronic components microelectronics. PSA tapes have been employed for the attachment of printed circuit boards to aluminum of copper to heat sinks as shown in Fig. 1, and found in automotive applications [2]. In such application, PSA is designed to resist flexural stress, and dampen noise and vibration. These adhesive are characterized by their shear and peel resistance as well as their initial tack. Additionally, PSA improved the assembly time, eliminate the need for mechanical joints and accommodate mismatch in the coefficient of thermal expansion of the joint materials due to the interface compliance. The reliability of these adhesive in electronic components depends on the integrity of the various interfaces in the assembly. In view of establishing the reliability of PSA joints, both deformation characteristics and failure process of the joint under simulated operating conditions need to be quantified.

Electronic assemblies employing adhesive joints are subjected to complex loading including tensile, shear, bending and as well as fatigue and creep loading. Consequently, different dominant failure modes of the joint have been observed including cohesive, adhesive and combination of both mechanisms [3]. Since the cohesive strength of adhesive is much greater than the adhesive-to-metal interfacial strength, cohesive failure near the interface is desired for enhancing the interfacial adhesion. Cohesive failure describes cracking within the bond thickness while adhesive failure refers to interface de-bonding between the adherents and the adhesive phase. The strength of the adhesive joint and the corresponding failure mechanism are dictated by numerous factors, including inadequate surface roughening of the adherents, chemical contamination and operating environment of humidity and temperature. Reliability assessment of electronic assemblies requires an understanding of the potential degradation mechanisms influencing the reliability of the components with adhesive joints. The mechanical properties of these adhesive materials are sensitive to the rate of loading and deformation [3, 4]. Effect of strain rate on tensile and shear properties, and the failure process significantly influence the impact performance of components with adhesive joints. In addition, the nonlinear behavior of the adhesive materials under different rates of loading has been investigated [5].

The mechanical behavior of polymeric materials can be described using hyper-elastic models based on strain energy density function. The choice of hyper-elastic models depends on the application, corresponding variables and available experimental data to establish the material parameters. Commonly used hyper-elastic models to describe the relationship between deformation and energy are Mooney-Rivlin [6], Yeoh [7], Ogden [8] and Gent [9]. Mooney-Rivlin model is widely used in the calculations of elastic deformation, assuming that the shear modulus does not vary with the strain. Yeoh model, also called the reduced polynomial model uses higher order of the left Cauchy-Green deformation tensor to describe the medium to large deformation range of the materials. In addition, the model is able to predict the stress-strain behavior at different deformation modes from a simple uniaxial test data [10]. In this paper, Yeoh hyper-elastic model is selected in view of its applicability to wide range of deformation.

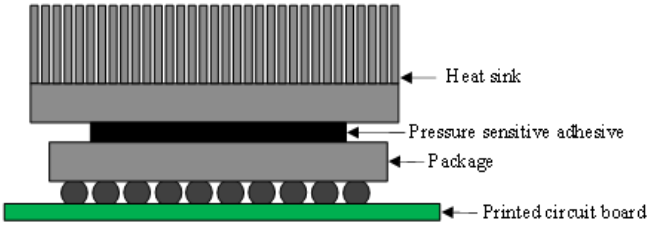

Fig.1. Schematic cross section of component-heat sink assembly with PSA joint.

The objective of this study is to establish strain rate-dependent deformation of PSA joints under tensile and shear loading. The applied displacement rates range from 5 to 500 mm/min. The corresponding failure modes of the adhesive joint are identified.

2. Material Modeling

Yeoh model is selected and evaluated using measured data for mechanical analysis of PSAs. Yeoh hyperelastic model express the strain energy density, W as express:

$$W = C_1(I_1 - 3) + C_2(I_1 - 3)^2 + C_3(I_1 - 3)^3 \qquad (1)$$

where $I_1 = \lambda_1^2 + \lambda_2^2 + \lambda_3^2$ with $\lambda_i (i = 1,2,3)$ denotes the stretch ratio in the three principal directions. The term λ_i is a material dimension expressed by $\lambda_i = L_i/L_{i0}$ wehere L_i and L_{i0} is the streched and initial length of the adhesive in the i^{th}-direction, respectively.

The coefficient C_1, C_2 and C_3 are material parameters determined using the uniaxial tensile data at specific temperature and stretching rate. The true stress, σ_1 is expressed in term of the stretch ratio based on Yeoh model in the tensile direction as:

$$\sigma_1 = 2(\lambda_1^2 - \frac{1}{\lambda_1})\left[C_1 + 2C_2\left(\lambda_1^2 + \frac{2}{\lambda_1} - 3\right) + 3C_3(\lambda_1^2 + \frac{2}{\lambda_1} - 3)^2\right] \qquad (2)$$

3. Materials and Experimental Procedures

The acrylic foam pressure sensitive adhesive (PSA) with thickness of 0.64 mm was used in the study (VHB 4930F supplied by 3M company). The adhesive pads were cut into circular samples with a diameter of 25 mm.

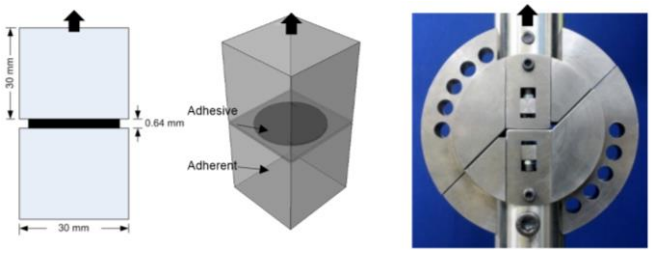

Fig. 2. Adhesively bonded specimen geometry and modified Arcan jig setup for tension test of the PSA specimen.

The bonded surfaces of aluminum adherents were abraded with #2000-grit SiC paper and then polished. The resulting surface roughness value of 0.012 µm was measured. The surfaces were degreased with acetone prior to the bonding process. A constant pressure of 137 kPa was applied for 15 seconds to the adhesively bonded specimen and left for 72 hours at room temperature before testing. A modified Arcan jig was used to apply tensile and pure shear loading to the specimen under different displacement rates of 5, 10, 50, 100, 250 and 500 mm/min. Schematic of the adhesively bonded specimen and the typical experimental setup for tension test is shown in Fig. 2. The orientation of the modified Arcan jig setup will enable various combinations of tensile and shear loading to be applied to the adhesive joint. The load-displacement response of the adhesively bonded specimen is recorded throughout the test to failure.

4. Finite Element Simulation

***Geometry and Boundary Conditions*:** Shear loading of the adhesive joints was simulated using finite element (FE) method. The geometry of the sample model was discretized into 106,820 8-node continuum elements. The adhesive region was discretized into finer element mesh in anticipation of the localized stress gradient, as shown in Fig. 3.

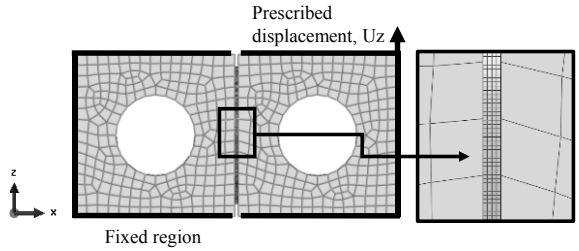

Fig. 3. Finite element model of the adhesive joints illustrating element mesh, boundary conditions and loading. (Shown in the 2D plane for the shear test).

5. Results and Discussion

Results are presented and discussed in terms of the mechanics of deformation, failure process of the adhesive joint and model validation for shear loading. The effects of loading rates on tensile and shear behavior of the adhesive joints are deliberated.

***Mechanics of deformation and failure process*:** Typical load-displacement responses of the adhesive joint under tensile and shear loading is shown in Fig. 4(a) and (b), respectively. Results show that the curve exhibits three distinct regimes of behavior. In the tensile deformation, the initial non-linear elastic response with homogeneous deformation is observed until the attainment of the peak load.

The deviation of the slope that signify the decrease in modulus is believed to coincide with the onset of the cavitation process at the adherent/adhesive interface. The reduction of the load bearing area due to the cavities leads to the observed decrease in load following the attainment of the peak value. The plateau and or/hardening region is characterized by fibrillation as the dominant failure mechanism. With continuously applied displacement, the

fibrillation process initiates and the adhesive material hardens as reflected in an increase in the load. Finally, the strained fibrils fracture as signified by the sudden drop in load.

In the shear loading of the adhesive joint, the initial stage relates to the bulk shearing of the adhesive confined between the aluminum adherents. With increasing shear displacement, fibrillation process initiates and the material stiffens until the peak load is reached. In this stage, the shear displacement of the adhesive joint is accommodated by a combination of fibrillation processes, shear flow, and interfacial sliding [11]. Finally, the fibrils fracture causing a sudden load drop in the load-displacement curve.

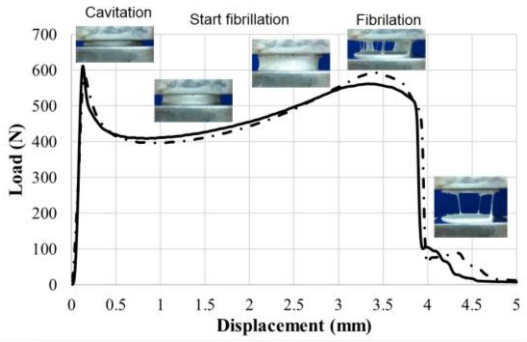

(a)

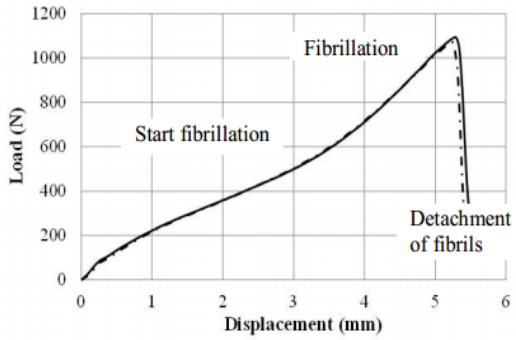

(b)

Fig 4. Load-displacement response of the adhesively bonded joint, illustrating the mechanisms of the failure process in (a) tensile and (b) shear loading. Dashed lines represent repeatability of the tests.

The tensile and shear strength of the adhesive joint is defined in this study as the peak load magnitude over the surface area of the pressure sensitive adhesive pad. The initial slope of the load-displacement curve is taken as the modulus of the adhesive joint while the area under the curve (per unit volume of the adhesive material) represents the strain energy density to fracture of the joint. The effects of deformation rate on these properties are discussed in the next section.

***Effects of loading rates on behavior of the adhesive joint*:** The load-displacement curves for the adhesive joints at various displacement rates ranging from 5 to 500 mm/min. are shown in Fig. 5. Similar results on the effect of tensile and shear loading show that the peak load increases while displacement at fracture decreases with increasing loading rate. This is consistent with previous observations [5]. Hardening effect, as manifested in a subsequent increase in load following the fibrillation process is more pronounced at higher loading rates.

Fig. 6 shows the variations of adhesive joint strength and modulus with displacement rate. The strength of the pressure sensitive adhesive joint to aluminum adherents increases non-linearly from 0.56 to 1.92 MPa over the displacement rates from 5 to 500 mm/min., respectively as shown in Fig. 6(a). Cavity formation is retarded at faster deformation speed, resulting in higher apparent strength. A continuous increase of the modulus of the adhesive joints is displayed with increasing displacement rate up to 100 mm/min. However, the modulus values gradually decrease at faster loading rates. This observed deformation response of the adhesive joint has been attributed to the polymer microstructure at high loading rate [12].

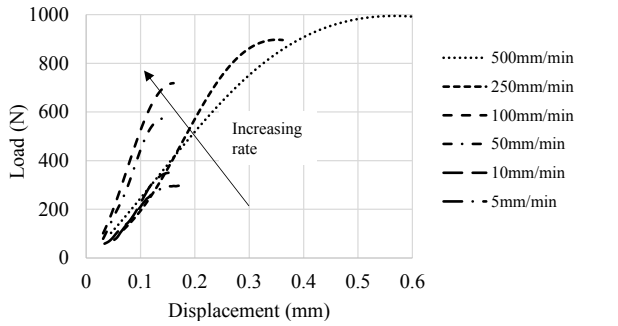

(a)

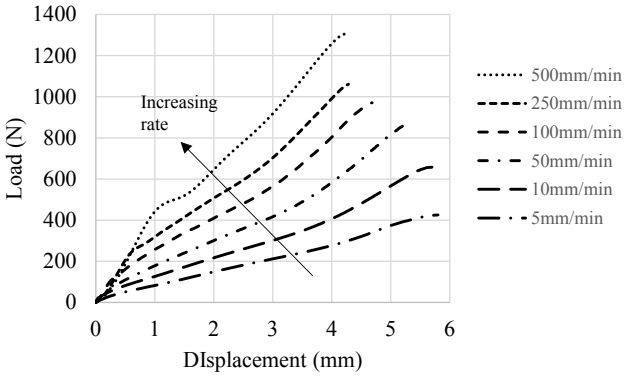

(b)

Fig. 5. Load-displacement plots up to peak load for (a) tensile and (b) shear loading.

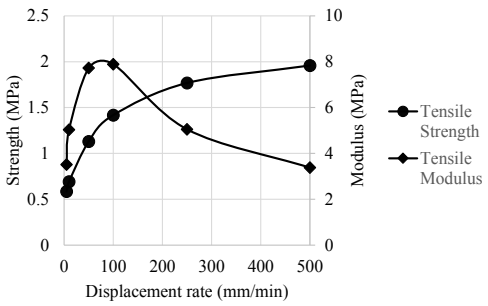

(a)

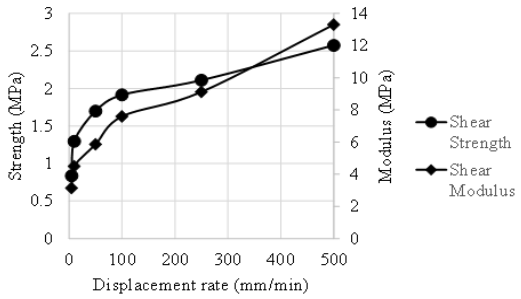

(b)

Fig. 6. Strength properties at fracture of the adhesive joint with displacement rates for (a) tensile and (b) shear loading.

In the shear loading of adhesive joints, the displacement rates has a significant effect on the shear strength and modulus, which increases proportionally with the displacement rates. The shear strength of the adhesive joint is measured as the maximum shear force per unit bonded area and represents the resistance of the adhesive joint to the shear stress.

The calculated strain energy density at fracture as a function of displacement rates is shown in Fig. 7. In the tensile loading, a decrease of modulus at high loading rate should be of concern when considering the performance of the adhesive joints under impact loading. The energy density increases with the displacement rate to a maximum magnitude of 5.7 N.mm/mm^3 at around 200 mm/min. and slightly decreases at higher displacement rates. The energy is dissipated primarily through fibrillation process of the adhesive joint. Results indicate that the pressure sensitive adhesive examined in this study is best for application involving quasi-static and low strain rates where both modulus and toughness of the adhesive joint is optimum (at around 100 mm/min.). Meanwhile, for the shear loading, the strain energy density increases with increase shear displacement. The effect of rate dependency on strength, modulus and strain energy density can be correlated with the speed of the motion of the molecular structure in a pressure sensitive adhesive at particular loading direction.

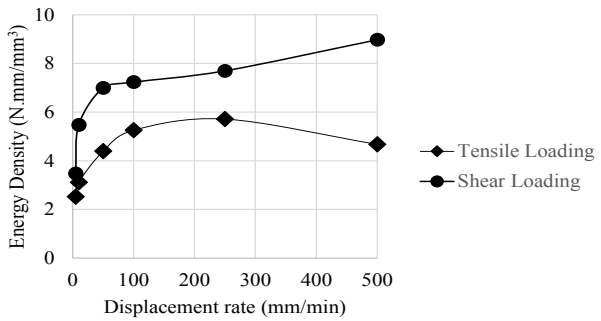

Fig. 7. Strain energy density at fracture of the adhesive joint with displacement rates.

***Rate-dependent failure modes*:** The tensile and shear failure modes of this pressure sensitive adhesive joint significantly depend on the rate of deformation. Fig. 8 identifies the dominant mode of failure observed when the adhesive joints is loaded at different rates of displacement and modes of loading.

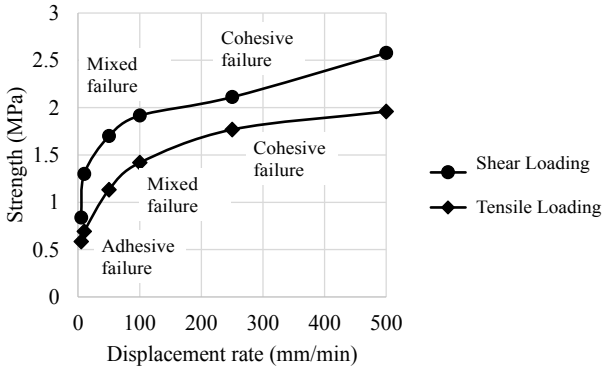

Fig. 8. Rate-dependent failure modes of the adhesive joints.

The fractured surface morphology was identified following the final failure where cohesive, adhesive and mixed-mode failure can be differentiated. In the tensile loading, adhesive failure dominates at slow loading rates between 5 to 10 mm/min, likely due crack propagating from the edge of the adherent/adhesive interface under the equilibrium stress concentration. In addition, the corresponding relatively low energy density results in adhesive failure due to the inability of the polymer to form a fibrillar structure [13]. Meanwhile no adhesive failure was observed under shear loading while mixed-mode failure dominates from 5 to 100 mm/min. At much faster rates of 250 and 500 mm/min. for the both loading cases, fibrillation of the adhesive joint dominates leading to the cohesive failure. A transition mode of failure is observed between these loading rate extremities.

***FE model validation*:** The FE simulation results in terms of the reaction force versus displacement of the adhesive joints are compared with measured data as shown in Fig. 9. A reasonably good correlation is demonstrated. Yeoh hyper-elastic material constitutive model is suitable to represent the viscous shear deformation of the joint for the shear loading rate to failure up to 250 mm/min. This comparison serves as a validation for the FE model.

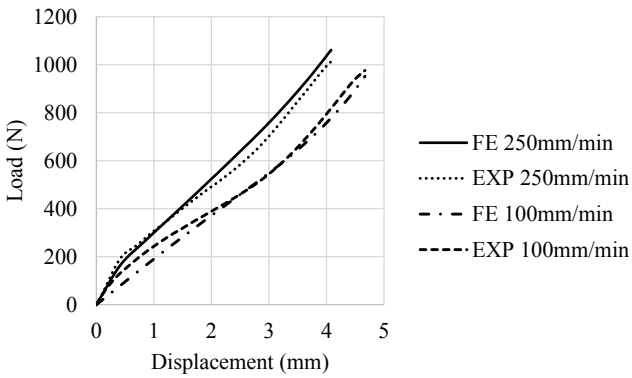

Fig. 9. Comparison of experimental and FE simulated load-displacement response of adhesive joints.

***Shear strain evolution in the adhesive joint*:** The evolution of the predicted shear strain in the PSA, τ_{13} for the shear displacement rate of 100 and 250 mm/min. is compared in Fig. 10. The magnitude of the shear strain is taken for the element at the critical edge location in the mid-plane of the adhesive pad. The relatively slow loading speed of 100 mm/min. allows the molecular structure of the polymer adhesive to deform to a greater peak strain magnitude of 132 pct. when compared to that at 250 mm/min. However, comparable shear strain level is achieved at the end of the simulated time that corresponds to the observed onset of the failure event. Such high strain at failure (~105 pct.) is associated with the dominant cohesive failure mechanism observed under shear loading.

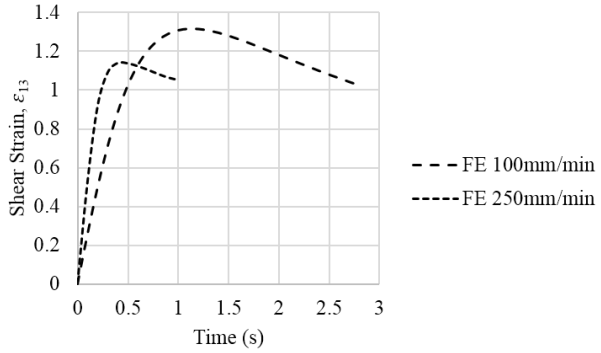

Fig. 10. Evolution of shear strain at the critical point in the PSA joint for different rates of loading.

6. Conclusions

Rate-dependent deformation response and failure process of pressure sensitive adhesive joint for aluminum adherents have been quantified experimentally under tensile and shear loading rates up to 500 mm/min. Results show that:

- The failure process under tensile loadings start with initiation of cavities, hardening through fibrillation process and final fracture of the fibrils. For shear loading the failure process is a combination of fibrillation processes, shear flow, and by interfacial sliding.
- Both modulus and strain energy density at fracture reach maximum value at a displacement rate of 100 mm/min under tension, while continuously increase with displacement rate under shear loading.
- Adhesive failure dominates at low loading rate (below 10 mm/min.), while mixed and cohesive failure is prominent at faster loading rates above 250 mm/min.
- Finite element simulation with Yeoh constitutive model adequately predicts the viscous shear deformation of adhesive joints.

Acknowledgment. This work is supported by the Ministry of Education Malaysia and Universiti Teknologi Malaysia through the Flagship Research University Grant No. 00G42.

References

1. Eveloy, V., Rodgers, P. and Pecht, M. G., "Reliability of Pressure-Sensitive Adhesive Tapes for Heat Sink Attachment in Air-Cooled Electronic Assemblies," *IEEE Transactions on Device and Material Reliability*, Vol. 4, No. 4 (2004), pp. 650-657.
2. Lall, P., Islam, N., Shete, T., Evans, J., Suhling, J., Gale, S., "Damage Mechanics of Electronics on Metal-Backed Substrates in Harsh Environments," *Proc. 54th Electronic Components and Technology Conf,* 2004, pp. 704-711.
3. Townsend, B. W., Ohanehi, D. C., Dillard, D. A., Austin, S. R., Salmon, F., Gagnon, D. R., "Characterizing Acrylic Foam Pressure Sensitive Adhesive Tapes for Structural Glazing Applications-Part I: DMA and Ramp-to-Fail Results," *International Journal of Adhesion and Adhesives,* Vol. 31, No. 7 (2011), pp. 639-649.
4. Gilat, A., Goldberg, R. K., and Roberts, G. D., "Strain Rate Sensitivity of Epoxy Resin in Tensile and Shear Loading," *Journal of Aerospace Engineering,* Vol. 20, No. 2 (2007), pp. 75-89.
5. Hennage, J., Characterization of a Pressure Sensitive Adhesive (PSA) for Mechanical Design. 2004, *Master Thesis*. Virginia Polytechnic Institute and State University.
6. Mooney, M., "A Theory of Large Elastic Deformation," *Journal of Applied Physics,* Vol. 11, No. 9 (1940), pp. 582-592.
7. Yeoh, O. H., "Characterization of Elastic Properties of Carbon-Black-Filled Rubber Vulcanizates," *Rubber Chemistry and Technology,* Vol. 63, No. 5 (1990), pp. 792-805.
8. Dorfmann, A. and Ogden, R., "Nonlinear Electroelasticity," *Acta Mechanica,* Vol. 174, No. 3-4 (2005), pp. 167-183.
9. Boyce, M. C. and Arruda, E. M., "Constitutive Models of Rubber Elasticity: A Review," *Rubber Chemistry and Technology,* Vol. 73, No. 3 (2000), pp. 504-523.
10. Ali, A., Hosseini, M. and Sahari, B., "A Review of Constitutive Models for Rubber-like Materials," A*merican Journal of Engineering and Applied Sciences,* Vol. 3, No. 1 (2010), pp. 232.
11. Sekine, S. and Kawakatsu, T., "Simple Crack Propagation Model of Pressure-Sensitive Adhesives," *Advances in Natural Sciences: Nanoscience and Nanotechnology,* Vol. 4, No. 2 (2013), pp. 025016.
12. Stenzler, J. S. and Goulbourne, N., Effect of Polyacrylate Interlayer Microstructure on the Impact Response of Multi-Layered Polymers, in Time Dependent Constitutive Behavior and Fracture/Failure Processes, Volume 3, Springer (New York, 2011), pp. 241-258.
13. Chang, E. P., "Viscoelastic Windows of Pressure-Sensitive Adhesives," *The Journal of Adhesion,* Vol. 34, No. 1-4 (1991), pp. 189-200.